Pure Appl. Chem., Vol. 84, No. 6, pp. 1455–1467, 2012.
http://dx.doi.org/10.1351/PAC-CON-11-09-02

Conformationally constrained and nanoparticle-targeted paclitaxels*

David G. I. Kingston[1,‡], Lawrence Tamarkin[2], and Giulio F. Paciotti[2]

[1]Department of Chemistry, Virginia Tech, Blacksburg, VA 24061, USA; [2]CytImmune Sciences, Inc., 105010 Broschart Rd., Rockville, MD 20850, USA

Abstract: Paclitaxel (Taxol®) is one of the most important anticancer agents developed over the last 30 years. Its primary mechanism of action is by interaction with the cellular protein tubulin, causing irreversible polymerization to microtubules. A detailed knowledge of this crucial interaction is thus of paramount importance in the design and development of highly potent analogs and also for the potential development of "non-taxane" tubulin polymerization agents. This review briefly describes the discovery and development of taxol, and then describes our work on delineating the tubulin-binding conformation of paclitaxel by a combination of rotational echo double resonance (REDOR) NMR and molecular modeling. The resulting "T-taxol" conformation was validated by the synthesis of conformationally constrained paclitaxel analogs, which had bioactivities up to 20-fold higher than those of paclitaxel. The review concludes with recent work on the development of a gold nanoparticle derivative of paclitaxel. This delivery method has the potential to lower the dosage of paclitaxel needed while maintaining or increasing its effectiveness, thus significantly improving the benefits of this important chemotherapeutic agent.

Keywords: gold nanoparticles; natural products; paclitaxel.

INTRODUCTION

The discovery of the anticancer diterpenoid taxol (now known as paclitaxel)** marked a new phase in the development of cytotoxic cancer chemotherapeutics, since it ushered in a new mechanism for cell death and provided one of the most effective anticancer drugs of the last half-century. The story of paclitaxel's discovery and development has been told many times [1,2], and so it will only be summarized briefly here. The original collection of bark from the western yew, *Taxus brevifolia*, was made in 1962, and the structure of paclitaxel (**1**) was published by Wall and Wani in 1971; a key part of the structure elucidation was the X-ray crystallographic work by Andrew McPhail at Duke University [3]. The final structure revealed paclitaxel to consist of a phenyl isoserine side chain linked to the C-13 position of the known compound baccatin III.

The initial report on paclitaxel's structure and activity was met with underwhelming enthusiasm, primarily because of the obvious problems of compound supply and solubility. Fortunately, scientists at the National Cancer Institute (NCI) continued to investigate the promising lead, and in the mid-1970s found that it was active against solid tumors, including some human tumor xenografts in nude mice.

Pure Appl. Chem.* **84, 1297–1478 (2012). A collection of invited papers based on presentations at the 27th International Symposium on the Chemistry of Natural Products and the 7th International Conference on Biodiversity (ISCNP-27 & ICOB-7), Brisbane, Australia, 10–15 July 2011.

‡Corresponding author

**The name Taxol has been trademarked by Bristol-Myers Squibb for their formulation of the compound named taxol by its discoverers.

This led to the decision by the NCI in 1977 to begin preclinical development of paclitaxel, a decision supported by observation of strong activity against the MX-1 mammary and CX-1 colon xenograft models of human solid tumors.

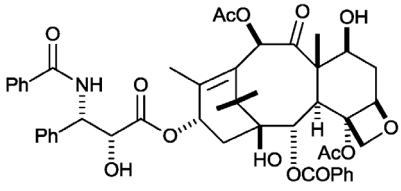

1 Paclitaxel

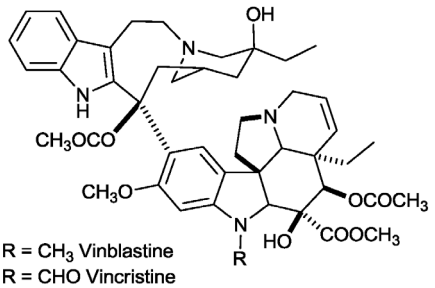

2 R = CH_3 Vinblastine
3 R = CHO Vincristine

A major breakthrough in paclitaxel's development came in 1979 with the report of its unprecedented activity as a tubulin polymerization agent. Although several compounds, including the clinically used agents vinblastine and vincristine (**2** and **3**), were known to prevent the polymerization of tubulin to functional microtubules, paclitaxel was the first compound known to promote this transformation. This discovery was crucial in raising interest in paclitaxel as a potential drug, and led indirectly to its eventual approval by the U.S. Food and Drug Administration for treatment of ovarian cancer in December 1992 and later for treatment of metastatic breast cancer in 1994; it was initially marketed as Taxol® by Bristol-Myers Squibb under an Orphan Drug designation, but is now a generic drug. The work leading to the clinical approval of paclitaxel has been summarized by Suffness [4], who was one of the key supporters of its development within the NCI.

Since the introduction of paclitaxel, two additional compounds have been introduced into clinical use. Docetaxel (**4**) was introduced by Rhone-Poulenc (now Sanofi-Aventis) as a semisynthetic analog of paclitaxel in 1994, and cabazitaxel (**5**) was introduced in 2010, also by Sanofi-Aventis, for the treatment of hormone-refractory metastatic prostate cancer. Several other paclitaxel analogs and prodrugs are also in clinical trials, and it is probable that additional analogs will be approved for clinical use in the future [5].

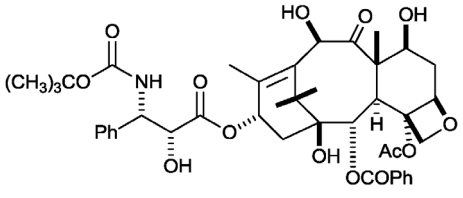

4 Docetaxel

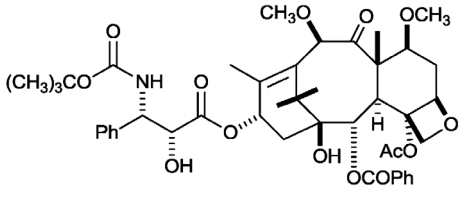

5 Cabazitaxel

THE TUBULIN-BINDING STRUCTURE OF PACLITAXEL

Biochemistry

Cell division, one of the key parts of cancer growth and progression, involves a carefully controlled sequence of events in which the parent cell passes through various phases on its way to mitosis, or cell division. The premitotic parts of the cell cycle are termed the G_1 phase, the S phase, and the G_2 phase. A very simplified summary of a complex process is that in the G_1 phase the cell synthesizes the various enzymes needed for mitosis, in the S phase DNA synthesis occurs leading to replication of all the

chromosomes, and in the G_2 phase microtubules are formed from the protein tubulin. The microtubules are key to the mitotic phase, in which the chromosomes of the two daughter cells are separated to form part of the nuclei of the new cells.

Microtubules are hollow tubes assembled dynamically from the proteins α- and β-tubulin, together with various microtubule-associated proteins (MAPs). The normal process of microtubule assembly is reversible, proceeding through α,β-dimers and oligomers to a fully assembled microtubule with 13 protofilaments and a diameter of 24 nm (Fig. 1a). The reversibility of microtubule assembly and disassembly is a key factor in the function of physically moving the chromosomes to form the nuclei of two daughter cells, since the resulting microtubules can grow and shrink and move within the cell.

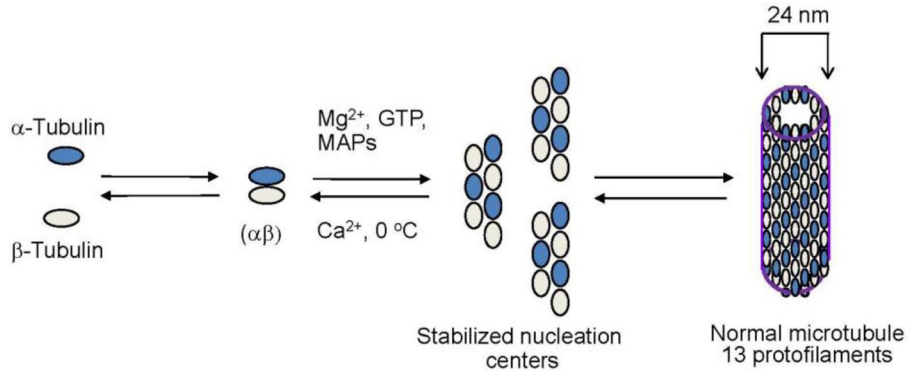

Fig. 1a Normal microtubule assembly from α- and β-tubulin.

In the presence of paclitaxel this reversible assembly is disrupted. Paclitaxel binds to the assembled microtubule in an approximate ratio of one molecule of paclitaxel per tubulin dimer [6], and induces the formation of stable but abnormal microtubules with 12 instead of 13 protofilaments (Fig. 1b). This disruption of the equilibrium leads to cell dysfunction and cell death by apoptosis [7]. The binding of paclitaxel to tubulin in microtubules is thus the key mechanism of its action as an anticancer agent.

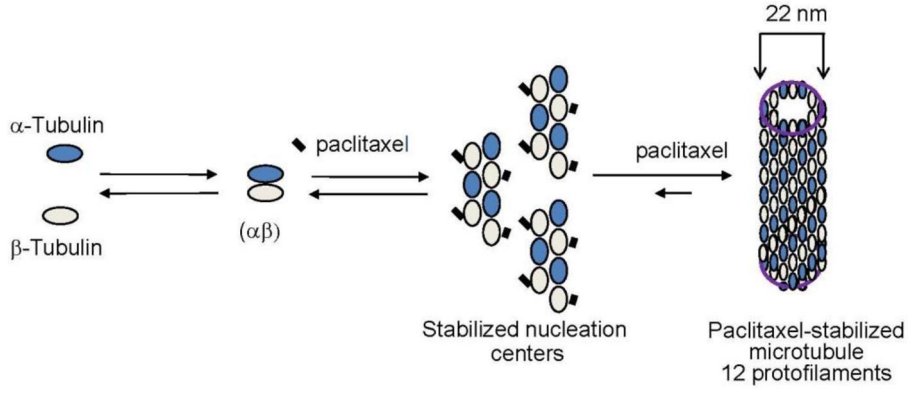

Fig. 1b Abnormal microtubule assembly from α- and β-tubulin in the presence of paclitaxel.

The paclitaxel–tubulin interaction

Because of the importance of the binding of paclitaxel to tubulin, many scientists have studied it in various ways. Since tubulin cannot be crystallized, a direct X-ray study is not possible, but information on the position of binding was initially obtained by photoaffinity labeling. These studies showed that paclitaxel binds to β-tubulin, with labeling occurring at the N-terminal 31 amino acids [8], amino acid residues 217–231 [9], or at the Arg^{282} position [10], depending on the photoaffinity analog used. These studies were confirmed and extended by important electron crystallography studies on zinc sheets of tubulin, which were ultimately carried out at a resolution of 3.5 Å [11]. These studies confirmed the location of the paclitaxel-binding region on β-tubulin in the microtubule, but were not able to reveal any information on the conformation of paclitaxel in the binding site.

The tubulin-binding conformation of paclitaxel

A knowledge of the binding conformation of paclitaxel on the assembled microtubule is of great interest, because it could in principle lead to the design of constrained analogs with this conformation built in, thus reducing the entropic cost of freezing out many of the rotational degrees of freedom inherent in the side chains of paclitaxel. It could also in principle lead to the design of simplified analogs of paclitaxel which had the correct shape for binding to and stabilizing microtubules.

Several proposals for the tubulin-binding conformation of paclitaxel have been made over the past 15 years. Two early proposals were based on nuclear Overhauser enhancement spectroscopy (NOESY) NMR studies of paclitaxel in solution; studies in chloroform gave rise to a "nonpolar" conformation [12–14], while studies in aqueous dimethyl sulfoxide (DMSO) indicated a "polar" conformation [15,16]. A later study discovered several possible conformations of paclitaxel in chloroform by the use of the NMR analysis of molecular flexibility in solution (NAMFIS) method, and among these was the previously undetected T-taxol conformation [17]. Examples of these conformations are shown in Fig. 2.

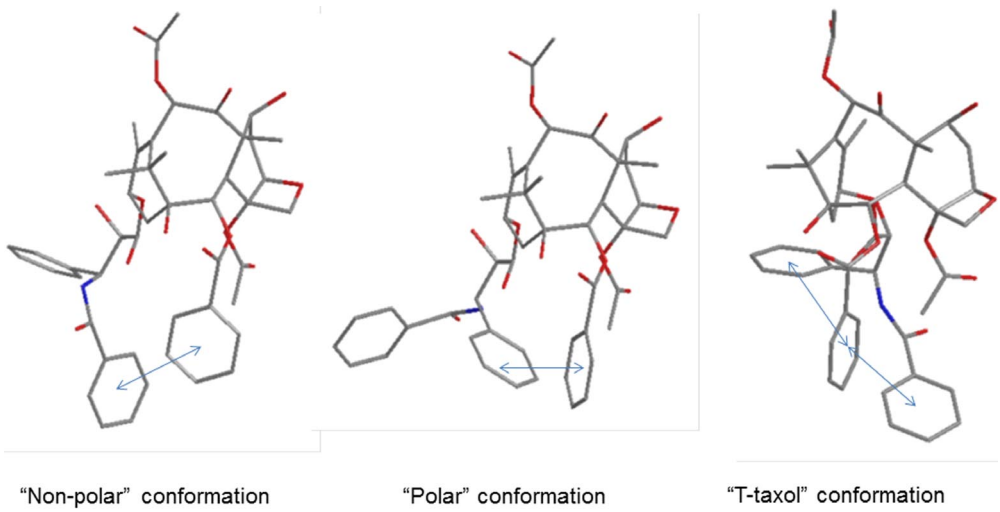

Fig. 2 Examples of "nonpolar", "polar", and "T-taxol" conformations of paclitaxel.

All of these conformations were based on NMR studies in solution, whereas the conformation desired is that of paclitaxel on the solid microtubule polymer. Fortunately, the relatively new technique of rotational echo double resonance (REDOR) NMR was developed for just such a situation. REDOR NMR is a spectroscopic technique for solids spinning at the magic angle, so it can be used for ligand-

bound microtubules. It provides a direct measurement of heteronuclear dipolar coupling between pairs of labeled nuclei, and distances of up to 12 Å can be determined with 0.5 Å accuracy [18].

Synthesis of labeled paclitaxels and evaluation by REDOR NMR

REDOR NMR requires the use of isotopically labeled compounds, so that the signals from the ligand can be distinguished reliably from the signals due to the protein. In the case of paclitaxel, where the distances between the C-13 side chain and the tetracyclic ring system were of the greatest interest, this involved the synthesis of both labeled side chains and labeled ring systems. The labeled side chain was prepared as its β-lactam precursor, allowing the use of the Holton–Ojima method [19] for coupling to protected baccatin III (Scheme 1).

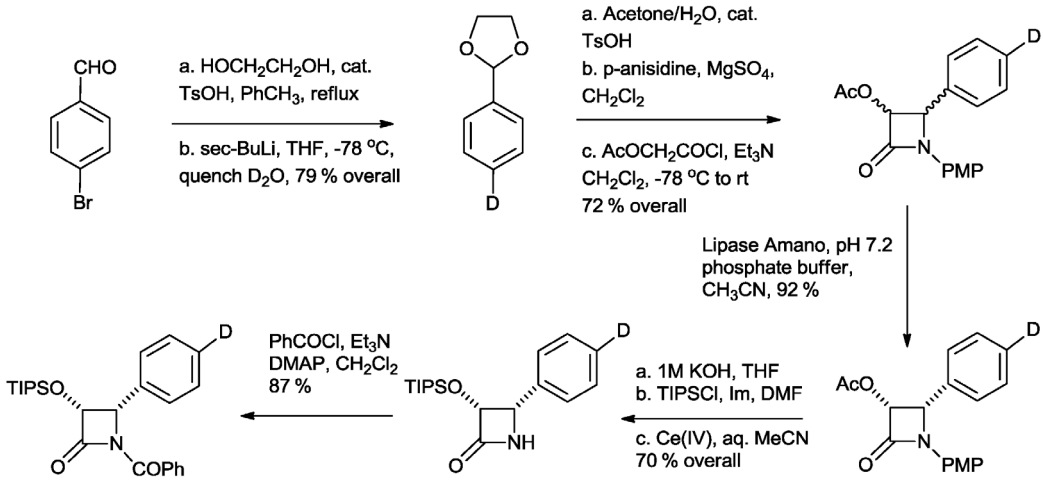

Scheme 1 Synthesis of a deuterium-labeled paclitaxel side chain for REDOR NMR analysis.

The available starting material 10-deacetylbaccatin III was then converted to 4-deacetyl-4-(2,2,2-trideuteroacetyl)-2-debenzoyl-2-(4-fluorobenzoyl)-baccatin III by the process shown in Scheme 2; the first two steps followed a literature procedure [20]. Finally, the β-lactam was coupled with the labeled baccatin III and the resulting product deprotected to give the labeled paclitaxel **7**. The labeled paclitaxels **6** and **8** were prepared by similar procedures.

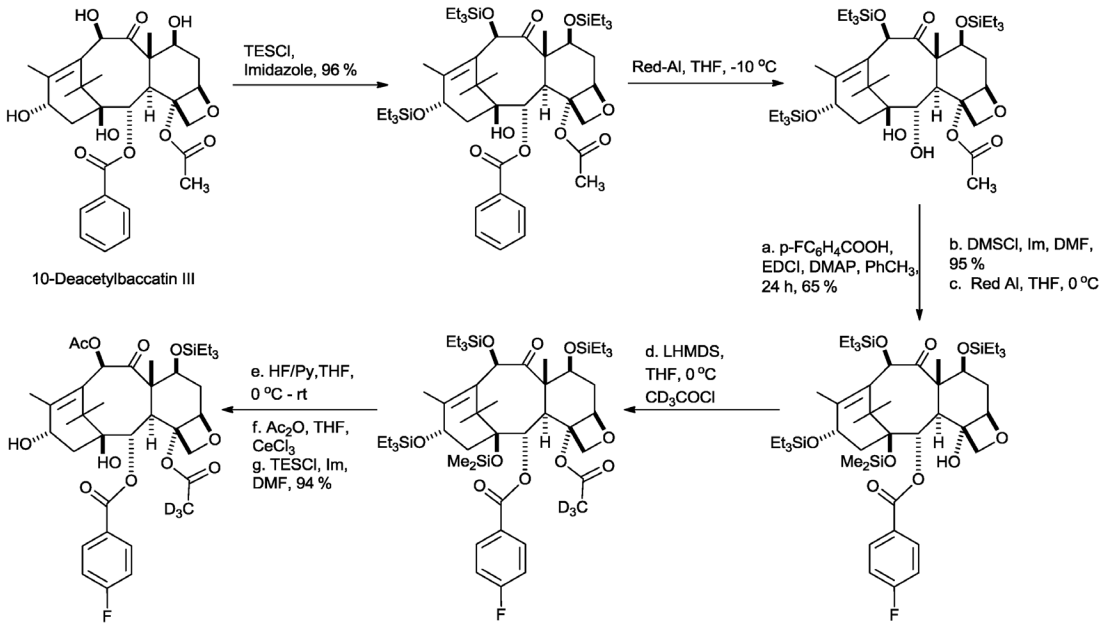

Scheme 2 Synthesis of a deuterium- and fluorine-labeled baccatin III for REDOR NMR analysis.

Once the three labeled paclitaxel analogs **6–8** were prepared, and Prof. Susan Bane at SUNY Binghamton used them to prepare microtubules, which were then shipped to Prof. Jake Schaefer at Washington University for analysis by REDOR NMR [21]. Once the inter-atomic distances were determined from the REDOR experiments (Fig. 3), these distances were then compared with the calculated distances for each of the three paclitaxel conformations described above (Table 1).

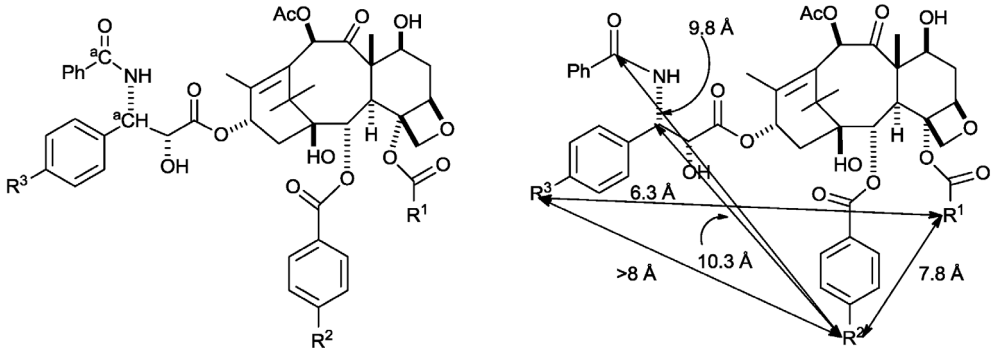

6 a = 13, $R^1 = CH_3$, $R^2 = F$, $R^3 = H$
7 a = 12, $R^1 = CD_3$, $R^2 = F$, $R^3 = D$
8 a = 12, $R^1 = CD_3$, $R^2 = H$, $R^3 = F$

Fig. 3 Labeled paclitaxels and the inter-atomic distances from REDOR experiments.

Examination of Table 1 indicates that the T-taxol conformation is the one that fits the experimental distances the best. The two other conformations each had at least one inter-nuclear distance outside the experimental error of the REDOR technique (±0.5 Å). These results thus established the T-taxol conformation as the closest model of the tubulin-binding conformation of paclitaxel.

This determination of the T-taxol conformation revealed a unique opportunity to test the validity of the assignment to an experimental test. This is an important consideration, because the electron diffraction structure of tubulin was obtained on zinc sheets [11], not on microtubules, and the possibility always existed that the structure of the protein in microtubules differed significantly from its structure on zinc sheets.

Table 1 Comparison of calculated and experimental inter-atomic distances for three models of the conformation of paclitaxel.

		Distances, Å			
Separation	Cmpd	Nonpolar model	Polar model	T-taxol model	REDOR distance
R^2-CH	**6**	8.5	**9.6**	**9.9**	10.3
R^2-C	**6**	6.2	**10.4**	**9.1**	9.8
R^2-R^3	**7**	**12.5**	4.5	**12.2**	>8
R^1-R^2	**7**	**8.0**	**7.4**	**7.9**	7.8
R^1-R^3	**8**	7.2	**5.5**	**6.6**	6.3

Synthesis and biological evaluation of bridged paclitaxels

Inspection of the T-taxol conformation from a different perspective (Fig. 4) shows that the C4-OAc group and the C3'-phenyl ring are in reasonably close proximity. This immediately led to the design and synthesis of analogs of paclitaxel with bridging links between these two groups. After an initial false start in which the bridging linkage was attached to the *meta*-position of the phenyl ring [22], success was achieved with bridging linkages from the *ortho*-position of the phenyl ring to the C4-OAc group. A summary of the synthetic scheme used for one of these is shown in Scheme 3; the β-lactam **9** was prepared by a modification of the method of Scheme 1, and the baccatin III derivative **10** was prepared by a modification of the method of Scheme 2. The final macrocyclic ring closure was brought about by the well-established Grubbs' methathesis reaction. The final products were designated britaxels (for bridged paclitaxels), with the suffix designating the bridge length. Several other britaxels were prepared, and three other representative ones are shown in Fig. 5 [23,24].

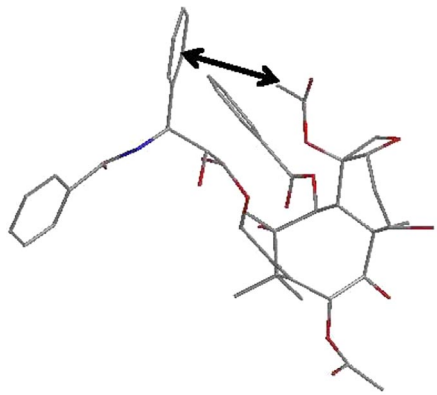

Fig. 4 T-taxol showing the close distance between the C4-OAc group and the C-3' phenyl group.

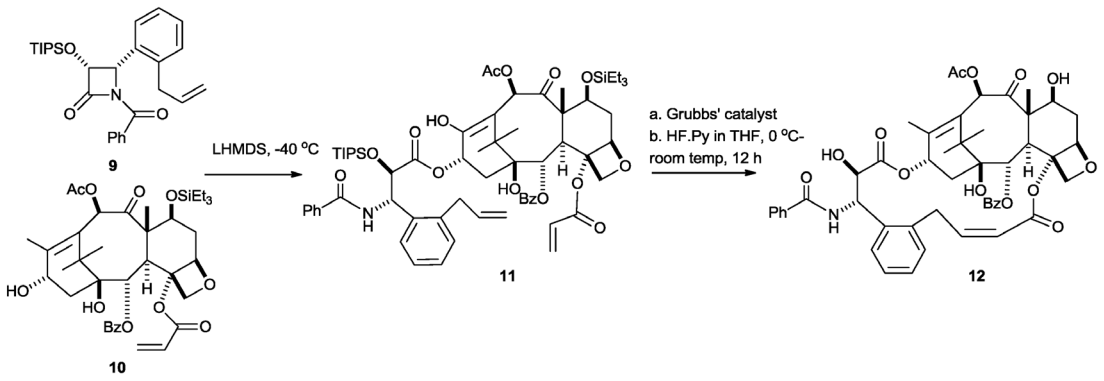

Scheme 3 Synthesis of britaxel-5 (**12**).

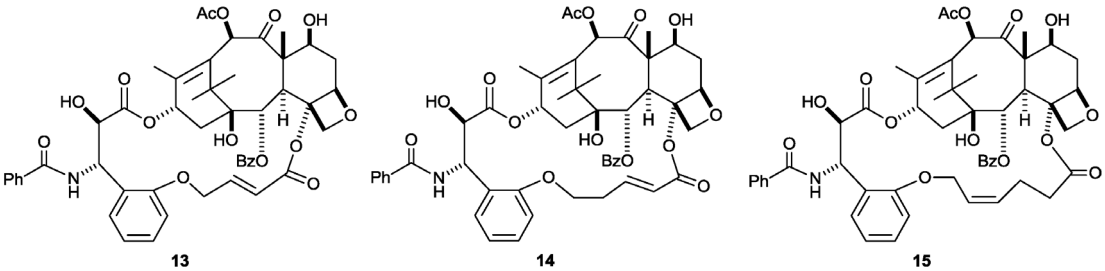

Fig. 5 Britaxels-6 (**13**), -7 (**14**), and -8 (**15**).

The biological activities of the britaxels were gratifyingly consistent with the conclusions from the REDOR data (Table 2).

Table 2 Bioactivity of britaxels **12–15**.

Compound	Tubulin polymerization (ED_{50}, μM)	IC_{50}, nM[b]		RR[c]
		1A9	1A9-PTX10	PTX10/1A9
Paclitaxel	0.5	4.8 ± 4.5	157	20
12	0.3	0.32 ± 0.35	0.13	1.8
13	0.28	7.0 ± 0.85	126	17
14	0.67	12.2 ± 7.0	157	9.2
15	ND	24.6 ± 9.0	196	6.3

Britaxel-5 (**12**), in particular, was significantly more potent than paclitaxel in the 1A9 ovarian cancer cell line, with an IC_{50} value approximately 15-fold lower than that of the natural product. Even more significant, britaxel-5 was over 100-fold more potent than paclitaxel in the paclitaxel-resistant cell line 1A9-PTX10 [24]. These data demonstrate the T-taxol conformation as the major tubulin-binding conformation of paclitaxel, and also validate the hypothesis that the paclitaxel binding sites are very similar in zinc sheets of tubulin and in microtubules.

Synthesis of bridged paclitaxel analogs

The validation of the T-taxol conformation then led naturally to the question of whether the bridging concept could be extended to increase the bioactivity of related compounds. In at least one case the answer was a resounding yes. The A-*nor*paclitaxel **16** was inactive against the A2780 ovarian cancer cell line, although it did retain some weak tubulin-assembly activity [25]. The bridged analog **17**, on the other hand, while less active than paclitaxel, did retain significant antiproliferative activity, and was actually superior to paclitaxel in its promotion of tubulin polymerization [26].

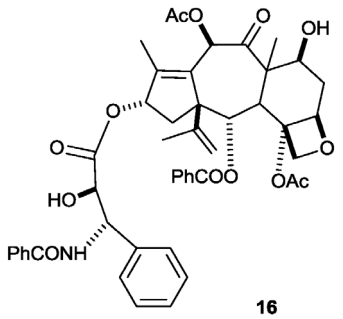

16

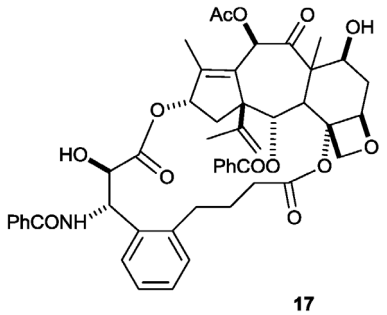

17

Attempts to design highly bioactive compounds that are greatly simplified analogs of paclitaxel using the T-taxol conformation as a guide have so far been only partially successful. Thus, both the derivatives **18** [27] and **19** [28] had some antiproliferative activity, but both were significantly less active than paclitaxel. The synthesis of analogs with modified structures that can mimic the T-taxol conformation and have similar bioactivities to those of paclitaxel has yet to be achieved.

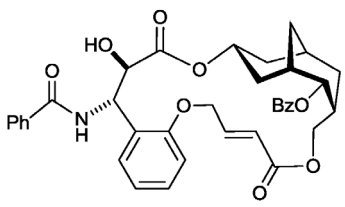

18

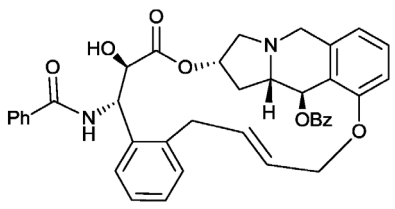

19

NANOPARTICLE-BASED DRUG DELIVERY OF PACLITAXEL

Classic cancer chemotherapy involves intravenous or oral administration of powerful cytotoxic drugs, resulting in severe side effects in many cases because the drug has little or no selectivity for cancer cells as opposed to normal cells. This problem can in principle be alleviated by the development of new drugs targeting specific enzymes, as for example with Gleevec [29], but this approach is very challenging, and success is likely to be limited to specific cancers, at least for the foreseeable future.

An alternative approach that can in principle lead to more rapid development of drugs with lower side effects is to develop specific targeted delivery methods for known and effective drugs such as paclitaxel, and this is the approach we have adopted. There are several good drug delivery strategies [30], including polymer-based nanoparticles [31] and gold nanoparticles; the latter having been used to construct delivery vehicles for oxaliplatin [32] and paclitaxel [33]. Nanoparticles are attractive drug-delivery vehicles because of the enhanced permeability and retention (EPR) effect, by which nanoparticles accumulate more rapidly in tumor tissues than in normal tissues. This effect is believed to be due to the

fact that the tumor neovasculature is formed quickly to provide increased blood supply to the growing tumor, and as such is ill-formed and "leaky". These leaky blood vessels coupled with a late-forming lymphatic system result in a net flow of fluids into the tumor which ultimately establishes a pressure gradient within the tumor. This pressure gradient, known as the interstitial fluid pressure gradient, acts as a physical barrier that limits the effective penetration of systemically administered chemotherapies within the tumor.

Our approach to the problem of delivering paclitaxel to tumors takes advantage of the EPR effect, but it complements this by adding tumor necrosis factor α (TNF) to the nanoparticle. TNF is a cytokine protein that is a critical component of the inflammatory immune cascade and also induces apoptotic cell death. In addition, TNF is a vascular disrupting agent, potentially breaking down tumor interstitial fluid pressure gradients, which might enhance the antitumor activity of subsequently administered chemotherapies.

However, TNF is too toxic to be administered systemically, although it has been used successfully in Europe in combination with melphalan for the treatment of bulky melanoma metastases and soft tissue sarcomas by the isolated limb perfusion technique [34]. TNF enhances tumor-selective drug uptake by inducing progressive vascular disruption within the tumor. A recent review [35] states "It now appears that treatment regimens that can limit the systemic destructive effects of TNF-alpha offer a viable therapeutic window to utilize TNF-alpha in patients." Our approach to achieving this goal was to mimic the regional perfusion paradigm described above by linking TNF and paclitaxel to the surface of the same colloidal gold nanoparticle.

The use of colloidal gold as a drug delivery vehicle for TNF has been reviewed, so this subject does not need to be discussed in depth [36]. The final nanoparticle construct is shown in Fig. 6. The central gold nanoparticle, approximately 27 nm in size, is formed by the classic Faraday technique of reducing a solution of gold chloride. The resulting nanoparticles are simultaneously derivatized with TNF, a paclitaxel derivative, and polyethylene glycol thiol (PEG-thiol), which reduces the probability of them being taken up by the mononuclear phagocytic system. This creates the final drug product [37].

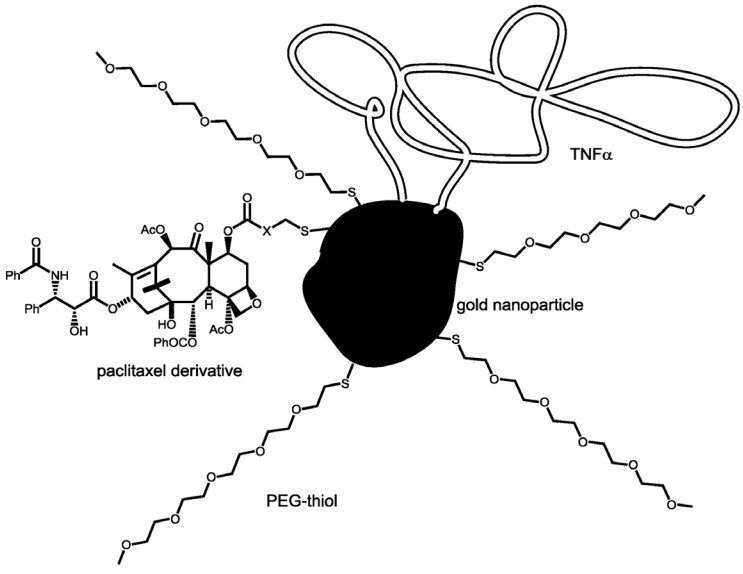

Fig. 6 Schematic representation of the nanoparticle-based delivery vehicle for paclitaxel.

Binding paclitaxel to gold nanoparticles requires that it be thiolated to allow formation of the strong, dative covalent gold–sulfur bond. Various paclitaxel analogs were prepared, and derivatives **20** and **21** were found to perform well, releasing paclitaxel from the nanoparticle at different rates.

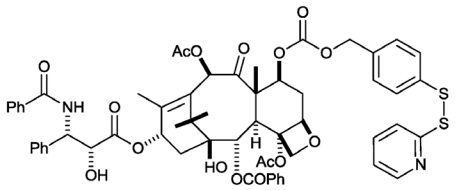

20

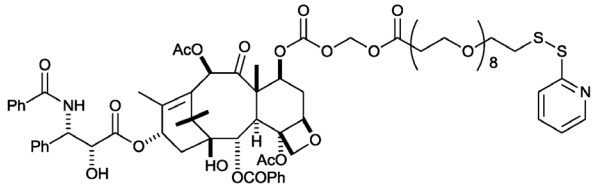

21

Although compounds **20** and **21** generate paclitaxel at different rates, we observed that once bound to gold the spontaneous rate of conversion of both analogs was reduced. We view such an effect as a benefit of the nanodrug as our preclinical data show only marginal release of the compounds in the circulation. Moreover, we observed that the nanoparticle drug sequestered significantly more drug within solid tumors when compared to native paclitaxel. Upon its arrival within the tumor we noted progressive generation of active drug over time.

The final validation of the efficacy of the nanoparticle delivery method was provided by an experiment with C57BL/6 mice bearing B16/F10 melanomas. For these studies, 1X105 B16/F10 tumor cells were implanted subcutaneously into female mice and allowed to grow until palpable tumors were detected. Animals presenting with tumors measuring 0.5 cm^3 were intravenously injected with either saline, native paclitaxel, or the gold nanoparticle construct. The animals were treated on days 0, 3, 5 and 7 of the study while tumor measurements were made before each treatment and on day 9 of the study.

Gold nanoparticles loaded with compound **20**, PEG-thiol, and TNF were used to treat tumor-burdened mice at a paclitaxel dose of 2.5 mg/Kg. In addition to untreated controls, paclitaxel at 40 and at 2.5 mg/Kg was used as a positive control. Paclitaxel at 2.5 mg/Kg was only marginally effective at reducing tumor volume as compared with untreated animals, but paclitaxel at 40 mg/Kg reduced tumor volume to approximately 28 % of that in the control group after nine days. The nanoparticle drug construct at 2.5 mg/Kg was almost as effective as paclitaxel at 40 mg/Kg, reducing tumor volume to approximately 32 % of that of the control group after nine days.

In summary, gold nanoparticles loaded with PEG-thiol, TNF, and compound **20** represent a novel nanotherapy that delivers two active pharmaceutical ingredients, TNF and paclitaxel, to solid tumors to produce a potent antitumor effect. The nanoparticles prevent the conversion to paclitaxel in the circulation, increasing the circulatory half-life of paclitaxel when compared to compound **20** and paclitaxel. Additionally, a combination of the passive EPR effect and the active binding of TNF to the tumor neovasculature actively sequesters the nanotherapy in solid tumors before it is subsequently converted to the active chemotherapy agent, paclitaxel. Thus, the gold nanoparticle drug construct represents an ideal nanomedicine capable of active tumor targeting, slowly releasing the active chemotherapy only at the site of disease.

ACKNOWLEDGMENTS

The synthetic work described in the first part of this paper was carried out by a group of talented graduate students and postdoctoral associates at Virginia Tech, including Thota Ganesh, Belhu Metaferia, Shoubin Tang, Chao Yang, and Jielu Zhao. The work would not have been possible without the outstanding collaboration of Jim Snyder and his group at Emory University, Susan Bane and her group at SUNY Binghamton, and Jake Schaefer and his group at Washington University, St. Louis. The work was supported by NIH grant CA69571, and this support is gratefully acknowledged. The nanoparticle

work described in the second part of the paper was supported by NIH SBIR grant CA119399 and by a State of Maryland Nanobiotechnology grant to CytImmune Sciences, Inc.

REFERENCES

1. G. M. Cragg, D. J. Newman. *J. Nat. Prod.* **67**, 232 (2004).
2. M. E. Wall. *Med. Res. Rev.* **18**, 299 (1998).
3. M. C. Wani, H. L. Taylor, M. E. Wall, P. Coggon, A. T. McPhail. *J. Am. Chem. Soc.* **93**, 2325 (1971).
4. M. Suffness, M. E. Wall. In *Taxol: Science and Applications*, M. Suffness (Ed.), pp. 3–25, CRC Press, Boca Raton (1995).
5. P. G. Mountford. In *Green Chemistry in the Pharmaceutical Industry*, P. J. Dunn, A. S. Wells, M. T. Williams (Eds.), pp. 145–160, Wiley-VCH (2010).
6. J. J. Manfredi, S. B. Horwitz. *Pharmacol. Ther.* **25**, 83 (1984).
7. L. A. Amos. *Org. Biomol. Chem.* **2**, 2153 (2004).
8. S. Rao, N. E. Krauss, J. M. Heerding, C. S. Swindell, I. Ringel, G. A. Orr, S. B. Horwitz. *J. Biol. Chem.* **269**, 3132 (1994).
9. S. Rao, G. A. Orr, A. G. Chaudhary, D. G. I. Kingston, S. B. Horwitz. *J. Biol. Chem.* **270**, 20235 (1995).
10. S. Rao, L. He, S. Chakravarty, I. Ojima, G. A. Orr, S. B. Horwitz. *J. Biol. Chem.* **274**, 37990 (1999).
11. J. Lowe, H. Li, K. H. Downing, E. Nogales. *J. Mol. Biol.* **313**, 1045 (2001).
12. J. Dubois, D. Guenard, F. Gueritte-Voeglein, N. Guedira, P. Potier, B. Gillet, J.-C. Betoeil. *Tetrahedron* **49**, 6533 (1993).
13. H. J. Williams, A. I. Scott, R. A. Dieden, C. S. Swindell, L. E. Chirlian, M. M. Francl, J. M. Heerding, N. E. Krauss. *Tetrahedron* **49**, 6545 (1993).
14. R. E. Cachau, R. Gussio, J. A. Beutler, G. N. Chmurny, B. D. Hilton, G. M. Muschik, J. W. Erickson. *Supercomp. App. High Perform. Comput.* **8**, 24 (1994).
15. D. G. Vander Velde, G. I. Georg, G. L. Grunewald, C. W. Gunn, L. A. Mitscher. *J. Am. Chem. Soc.* **115**, 11650 (1993).
16. L. G. Paloma, R. K. Guy, W. Wrasidlo, K. C. Nicolaou. *Chem. Biol.* **1**, 107 (1994).
17. J. P. Snyder, N. Nevins, D. O. Cicero, J. Jansen. *J. Am. Chem. Soc.* **122**, 724 (2000).
18. T. Gullion, J. Schaefer. *J. Magn. Reson.* **81**, 196 (1989).
19. R. A. Holton, R. J. Biediger, P. D. Boatman. In *Taxol: Science and Applications*, M. Suffness (Ed.), pp. 97–121, CRC Press, Boca Raton (1995).
20. I. Ojima, S. Lin, T. Inoue, M. L. Miller, C. P. Borella, X. Geng, J. J. Walsh. *J. Am. Chem. Soc.* **122**, 5343 (2000).
21. Y. Paik, C. Yang, B. Metaferia, S. Tang, S. Bane, R. Ravindra, N. Shanker, A. A. Alcaraz, S. A. Johnson, J. Schaefer, R. D. O'Connor, L. Cegelski, J. P. Snyder, D. G. I. Kingston. *J. Am. Chem. Soc.* **129**, 361 (2007).
22. B. B. Metaferia, J. Hoch, T. E. Glass, S. L. Bane, S. K. Chatterjee, J. P. Snyder, A. Lakdawala, B. Cornett, D. G. I. Kingston. *Org. Lett.* **3**, 2461 (2001).
23. T. Ganesh, R. C. Guza, S. Bane, R. Ravindra, N. Shanker, A. S. Lakdawala, J. P. Snyder, D. G. I. Kingston. *Proc. Natl. Acad. Sci. USA* **101**, 10006 (2004).
24. T. Ganesh, C. Yang, A. Norris, T. Glass, S. Bane, R. Ravindra, A. Banerjee, B. Metaferia, S. L. Thomas, P. Giannakakou, A. A. Alcaraz, A. S. Lakdawala, J. P. Snyder, D. G. I. Kingston. *J. Med. Chem.* **50**, 713 (2007).
25. G. Samaranayake, N. F. Magri, C. Jitrangsri, D. G. I. Kingston. *J. Org. Chem.* **56**, 5114 (1991).
26. S. Tang, C. Yang, P. Brodie, S. Bane, R. Ravindra, S. Sharma, Y. Jiang, J. P. Snyder, D. G. I. Kingston. *Org. Lett.* **8**, 3983 (2006).

27. T. Ganesh, A. Norris, S. Sharma, S. Bane, A. A. Alcaraz, J. P. Snyder, D. G. I. Kingston. *Bioorg. Med. Chem.* **14**, 3447 (2006).
28. J. Zhao, S. Bane, J. P. Snyder, H. Hu, K. Mukherjee, C. Slebodnick, D. G. I. Kingston. *Bioorg. Med. Chem.* **19**, 7664 (2011).
29. C. F. Waller. In *Recent Results in Cancer Research*, *Small Molecules in Oncology*, Vol. 184, Part 1, U. M. Martens (Ed.). Springer, Munich (2010).
30. J. L. Arias. *Mini Rev. Med. Chem.* **11**, 1 (2011).
31. M. E. Fox, F. C. Szoka, J. M. J. Frechet. *Acc. Chem. Res.* **42**, 1141 (2009).
32. S. D. Brown, P. Nativo, J.-A. Smith, D. Stirling, P. R. Edwards, B. Venugopal, D. J. Flint, J. A. Plumb, D. Graham, N. J. Wheate. *J. Am. Chem. Soc.* **132**, 4678 (2010).
33. J. R. Hwu, Y. S. Lin, T. Josephrajan, M.-H. Hsu, F.-Y. Cheng, C.-S. Yeh, W.-C. Su, D.-B. Shieh. *J. Am. Chem. Soc.* **131**, 66 (2009).
34. H. R. Alexander, D. L. Fraker, D. L. Bartlett. *Semin. Surg. Oncol.* **12**, 416 (1966).
35. D. Daniel, N. S. Wilson. *Curr. Cancer Drug Targ.* **8** (2008).
36. A. C. Powell, G. F. Paciotti, S. K. Libutti. *Methods Mol. Biol.* **624**, 375 (2010).
37. G. F. Paciotti, D. G. I. Kingston, L. Tamarkin. *Drug Dev. Res.* **67**, 47 (2006).

